

1 **Reactive processing of formaldehyde and acetaldehyde in**
2 **aqueous aerosol mimics: Surface tension depression and sec-**
3 **ondary organic products**

4 Z. Li, A. N. Schwier, N. Sareen, and V. F. McNeill*

5 Department of Chemical Engineering, Columbia University, New York, NY, 10027

6 *Correspondence to: V. Faye McNeill (vf2103@columbia.edu)

7 **Abstract**

8 The reactive uptake of carbonyl-containing volatile organic compounds (cVOCs) by
9 aqueous atmospheric aerosols is a likely source of particulate organic material. The aque-
10 ous-phase secondary organic products of some cVOCs are surface-active. Therefore,
11 cVOC uptake can lead to organic film formation at the gas-aerosol interface and changes
12 in aerosol surface tension. We examined the chemical reactions of two abundant cVOCs,
13 formaldehyde and acetaldehyde, in water and aqueous ammonium sulfate (AS) solutions
14 mimicking tropospheric aerosols. Secondary organic products were identified using Aero-
15 sol Chemical Ionization Mass Spectrometry (Aerosol-CIMS), and changes in surface ten-
16 sion were monitored using pendant drop tensiometry. Hemiacetal oligomers and aldol
17 condensation products were identified using Aerosol-CIMS. Acetaldehyde depresses sur-
18 face tension to $65(\pm 2)$ dyn cm^{-1} in pure water (a 10% surface tension reduction from that
19 of pure water) and $62(\pm 1)$ dyn cm^{-1} in AS solutions (a 20.6% reduction from that of a 3.1
20 M AS solution). Surface tension depression by formaldehyde in pure water is negligible;
21 in AS solutions, a 9% reduction in surface tension is observed. Mixtures of these species
22 were also studied in combination with methylglyoxal in order to evaluate the influence of
23 cross-reactions on surface tension depression and product formation in these systems. We
24 find that surface tension depression in the solutions containing mixed cVOCs exceeds that
25 predicted by an additive model based on the single-species isotherms.

26 **1 Introduction**

27 Organic material is a ubiquitous component of atmospheric aerosols, making up a ma-
28 jor fraction of fine aerosol mass, but its sources and influence on aerosol properties
29 are still poorly constrained (Jimenez et al., 2009; Kanakidou et al., 2005). Many
30 common organic aerosol species are surface-active (Facchini et al., 1999; Shulman et
31 al., 1996). Surface-active molecules in aqueous solution form structures that allow
32 hydrophobic groups to avoid contact with water while hydrophilic groups remain in
33 solution. In an aqueous aerosol particle, they may partition to the gas-aerosol inter-
34 face, reducing aerosol surface tension and potentially acting as a barrier to gas-aerosol
35 mass transport (Folkers et al., 2003; McNeill et al., 2006). Depressed aerosol surface
36 tension due to film formation may lead to a decrease in the critical supersaturation
37 required for the particle to activate and grow into a cloud droplet as described by Köh-
38 ler Theory (Kohler, 1936). The surface tension of atmospheric aerosol samples tends
39 to be lower than that predicted based on the combined effects of the individual surfac-
40 tants identified in the aerosol (Facchini et al., 1999). This is in part because some sur-
41 face-active aerosol organics remain unidentified. Additionally, the effects of interac-
42 tions among these species under typical aerosol conditions (i.e. supersaturated salt
43 concentrations, acidic, multiple organic species) are generally unknown.

44 The adsorption of volatile organic compounds (VOCs) to aqueous aerosol and
45 cloud droplet surfaces has been proposed as a route for the formation of organic sur-
46 face films (Djikaev and Tabazadeh, 2003; Donaldson and Vaida, 2006). There is also
47 growing evidence that the reactive uptake of the carbonyl-containing VOCs (cVOCs)
48 methylglyoxal and glyoxal by cloud droplets or aerosol water, followed by aqueous-
49 phase chemistry to form low-volatility products, is a source of secondary organic aer-
50 osol material (Ervens and Volkamer, 2010; Lim et al., 2010). We recently showed
51 that methylglyoxal suppresses surface tension in aqueous aerosol mimics (Sareen et
52 al., 2010).

53 Formaldehyde and acetaldehyde, two abundant, highly volatile aldehydes, can be
54 directly emitted from combustion and industrial sources or generated *in situ* via the

55 oxidation of other VOCs (Seinfeld and Pandis, 1998). In aqueous solution, both for-
56 maldehyde and acetaldehyde become hydrated and form acetal oligomers, similar to
57 methylglyoxal and glyoxal (Loudon, 2009) (see Figure S2 in the Supporting Infor-
58 mation for a schematic of the different reaction mechanisms discussed in this study).
59 Nozière and coworkers showed that acetaldehyde forms light-absorbing aldol conden-
60 sation products in aqueous ammonium sulfate solutions (Noziere et al., 2010a). For-
61 maldehyde was also recently suggested to react with amines to form organic salts in
62 tropospheric aerosols (Wang et al., 2010). Due to their prevalence and known aque-
63 ous-phase oligomerization chemistry, the reactive processing of these species in
64 aqueous aerosol mimics, alone and in combination with other cVOCs, is of interest,
65 but has not been thoroughly studied to date.

66 We investigated the chemical reactions of formaldehyde and acetaldehyde in pure
67 water and concentrated ammonium sulfate (AS) solutions mimicking aerosol water.
68 The potential of these species to alter aerosol surface tension was examined, and sec-
69 ondary organic products were identified using Aerosol Chemical Ionization Mass
70 Spectrometry (Aerosol-CIMS).

71 **2 Experimental Methods**

72 Aqueous solutions containing varying concentrations of organic compounds (ac-
73 etaldehyde, formaldehyde and/or methylglyoxal) with near-saturation concentrations
74 (3.1 M) of AS were prepared in 100 mL Pyrex vessels using Millipore water. The
75 concentration of formaldehyde used was 0.015 – 0.21 M. The concentration of acetal-
76 dehyde was 0.018 M – 0.54 M. In the preparations, 5 mL ampules of 99.9 wt% acet-
77 aldehyde (Sigma Aldrich) were diluted to 1.78 M using Millipore water immediately
78 after opening in order to minimize oxidization. Varying amounts of this stock solution
79 were used to prepare the final solutions within 30 minutes of opening the ampule.
80 Formaldehyde and methylglyoxal (MG) were introduced from 37 wt% and 40 wt%
81 aqueous solutions (Sigma Aldrich), respectively. The pH value of the reaction mix-
82 tures, measured using a digital pH meter (Accumet, Fisher Scientific), was 2.7-3.1.
83 The acidity of the solutions is attributable to trace amounts of acidic impurities within

84 the organic reagent stock solutions (i.e. pyruvic acid from the MG stock solution).

85 The surface tension of each sample was measured 24 hours after solution prepara-
86 tion using pendant drop tensiometry (PDT). Pendant drops were suspended from the
87 tip of glass capillary tubes using a 100 μ L syringe. The images of the pendant drops
88 were captured and analyzed to determine the shape factor, H , and equatorial diameter,
89 d_e , as described previously (Sareen et al., 2010; Schwier et al., 2010). These parame-
90 ters were used to calculate the surface tension according to:

$$91 \quad \sigma = \frac{\Delta\rho g d_e^2}{H} \quad (1)$$

92 where σ is surface tension, $\Delta\rho$ is the difference in density between the solution and the
93 gas phase, and g is acceleration due to gravity (Adamson and Gast, 1997). Solution
94 density was measured using an analytical balance (Denver Instruments). The drops
95 were allowed to equilibrate for 2 minutes before image capture. Each measurement
96 was repeated 7 times.

97 Aerosol-CIMS was used to detect the organic composition of the product mix-
98 tures as described in detail previously (Sareen et al., 2010; Schwier et al., 2010). Mix-
99 tures of formaldehyde, acetaldehyde-MG, and formaldehyde-MG in water and 3.1 M
100 AS were prepared. Total organic concentration ranged from 0.2-2 M. All the solutions
101 containing AS were diluted after 24 hours with Millipore water until the salt concen-
102 tration was 0.2 M. The solutions were aerosolized in a stream of N_2 using a constant
103 output atomizer (TSI) and flowed through a heated 23 cm long, 1.25 cm ID PTFE
104 tube (maintained at 135°C) at RH >50% before entering the CIMS, in order to volati-
105 lize the organic species into the gas phase for detection. The time between atomiza-
106 tion and detection is ≤ 3.5 s. Since the timescale for the oligomerization of these or-
107 ganics is on the order of hours (Sareen et al., 2010; Nozière et al., 2010a) the detected
108 molecules are most likely formed in the bulk aqueous solutions. The solutions were
109 tested in both positive and negative ion mode, using $H_3O^+ \cdot (H_2O)_n$ and I^- as reagent
110 ions, respectively. The applicability of this approach to the detection of acetal oligo-
111 mers and aldol condensation products formed by dicarbonyls in aqueous aerosol mim-

112 ics has been demonstrated previously (Sareen et al., 2010; Schwier et al., 2010). The
113 average particle concentration was $\sim 4 \times 10^4 \text{ cm}^{-3}$ and the volume weighted geometric
114 mean diameter was $414(\pm 14) \text{ nm}$.

115 The Pyrex vessels shielded the reaction mixtures from UV light with wavelengths
116 $< 280 \text{ nm}$ (Corning, Inc.), but the samples were not further protected from visible
117 light. We previously showed that exposure to visible light in identical vessels does not
118 impact chemistry in the glyoxal-AS or MG-AS reactive systems (Sareen et al., 2010;
119 Shapiro et al., 2009).

120 **3 Results**

121 **3.1 Surface Tension Measurements**

122 **3.1.1 Single-organic mixtures.** Results of the PDT experiments (Fig. 1) show that
123 both formaldehyde and acetaldehyde depress surface tension in 3.1 M AS solution,
124 but the formaldehyde mixture is less surface-active than that of acetaldehyde. The
125 formaldehyde-AS solutions reach a minimum surface tension of $71.4 \pm 0.4 \text{ dyn cm}^{-1}$ (a
126 9% reduction from that of a 3.1 M AS solution ($\sigma = 78.5 \pm 0.3 \text{ dyn cm}^{-1}$)), at 0.082 mol
127 $\text{C/kg H}_2\text{O}$. The acetaldehyde-AS solutions showed more significant surface tension
128 depression. The surface tension of the solutions reached a minimum of $62 \pm 1 \text{ dyn cm}^{-1}$
129 (a 20.6% reduction compared to 3.1 M AS solution), when the acetaldehyde concen-
130 tration exceeded $0.527 \text{ mol C/kg H}_2\text{O}$. Compared to the surface tension of the acetal-
131 dehyde in 3.1 M AS, the surface tension depression of acetaldehyde in water is less
132 significant. The surface tension of acetaldehyde in water decreases rapidly and reach-
133 es a minimum value of $65 \pm 2 \text{ dyn cm}^{-1}$ at $0.89 \text{ mol C/kg H}_2\text{O}$ (a 10% reduction from
134 that of pure water, 72 dyn cm^{-1}). Formaldehyde does not show any detectable surface
135 tension depression in water in the absence of AS.

136 The surface tension data can be fit using the Szyszkowski-Langmuir equation:

$$137 \sigma = \sigma_0 - aT \ln(1 + bC) \quad (2)$$

138 where σ and σ_0 are surface tension of the solution with and without organics, T is am-
139 bient temperature (298 K), C is total organic concentration (moles carbon per kg

140 H₂O), and a and b are fit parameters (Adamson and Gast, 1997). The parameters from
141 the fits to the data in Fig. 1 are listed in Table 1.

142 **3.1.2 Binary mixtures.** Surface tension results for aqueous solutions containing a
143 mixture of two organic compounds (MG and formaldehyde or acetaldehyde) and 3.1
144 M AS are shown in Fig. 2. For a given total organic concentration (0.5 or 0.05 M), the
145 surface tension decreased with increasing MG concentration. Re-plotting the data
146 from Fig. 2 as a function of MG concentration, it is apparent that the surface tension
147 was very similar for mixtures with the same MG concentration, regardless of the iden-
148 tity or amount of the other species present in the mixture (Fig. 3).

149 Henning and coworkers developed the following model based on the Szyszkow-
150 ski-Langmuir equation to predict the surface tension of complex, nonreacting mix-
151 tures of organics (Henning et al., 2005):

$$152 \quad \sigma = \sigma_0(T) - \sum_i \chi_i a_i T \ln(1 + b_i C_i) \quad (3)$$

153 Here, C_i is the concentration of each organic species (moles carbon per kg H₂O), χ_i is
154 the concentration (moles carbon per kg H₂O) of compound i divided by the total solu-
155 ble carbon concentration in solution, and a_i and b_i are the fit parameters from the
156 Szyszkowski-Langmuir equation for compound i . The Henning model has been
157 shown to describe mixtures of nonreactive organics, such as succinic acid-adipic acid
158 in inorganic salt solution, well (Henning et al., 2005). We also found that it was capa-
159 ble of describing surface tension depression in reactive aqueous mixtures containing
160 MG, glyoxal, and AS (Schwier et al., 2010).

161 The predicted surface tension depression for the binary mixtures as calculated
162 with the Henning model is shown in Fig. 2 as a black line, and the confidence inter-
163 vals based on uncertainty in the Szyszkowski-Langmuir parameters are shown in grey.
164 The experimentally measured surface tensions are, in general, lower than the Henning
165 model prediction, indicating a synergistic effect between MG and acetalde-
166 hyde/formaldehyde. The error of the prediction for the mixtures of MG and acetalde-
167 hyde is between 8-24%. The error tends to increase with the concentration of MG.
168 However, the error is less than 10% for formaldehyde-MG mixtures.

169 **3.1.3 Ternary mixtures.** As shown in Fig. 4, 3.1 M AS solutions containing ter-
170 nary mixtures of MG, acetaldehyde and formaldehyde also exhibit surface tension de-
171 pression lower than that predicted by the Henning model. For the ternary mixture ex-
172 periments, the molar ratio of acetaldehyde to formaldehyde was either 1:3 (Fig. 4a
173 and 4b) or 1:1 (Fig. 4c and 4d) and the MG concentration was varied. The total organ-
174 ic concentration remained constant at 0.05 M. Recasting the data of Fig. 4 as a func-
175 tion of MG concentration shows a similar trend as what was observed for the binary
176 mixtures; for a constant total organic concentration, MG content largely determines
177 the surface tension, regardless of the relative amounts of acetaldehyde and formalde-
178 hyde present (Fig. 3).

179

180 **3.2 Aerosol-CIMS characterization**

181 The CIMS data show products of self- and cross-reactions of formaldehyde, acetalde-
182 hyde and MG in pure water and 3.1 M AS. The resolution for all CIMS data presented
183 here was $m/z \pm 1.0$ amu. All the peaks identified and discussed in the following sec-
184 tions have signal higher than that present in a N_2 background spectrum. Any unlabeled
185 peaks are within the background, and were not included in the peak assignment analy-
186 sis. We did not perform Aerosol-CIMS analysis on acetaldehyde-AS or acetaldehyde-
187 H_2O solutions because these systems have been characterized extensively by others
188 (Casale et al., 2007; Noziere et al., 2010a). These studies showed the acid-catalyzed
189 formation of aldol condensation products in solutions containing AS.

190 **3.2.1 Formaldehyde.** The mass spectra for formaldehyde in H_2O and in 3.1 M AS
191 obtained using negative ion detection with I^- as the reagent ion is shown in Fig. 5.
192 Possible structures are shown in Table 2. The spectrum shows peaks with mass-to-
193 charge ratios corresponding to formic acid at 81.7 ($CHO_2^- \cdot 2H_2O$) and 208.7 amu (I^-
194 $\cdot CH_2O_2 \cdot 2H_2O$) and several peaks consistent with hemiacetal oligomers. 223.3, 291.1,
195 and 323.5 amu are consistent with clusters of hemiacetals with I^- . The peaks at 95.6,
196 110.4, 273.8 and 304.7 amu are consistent with clusters of ionized hemiacetals with
197 H_2O . While ionization of alcohols by I^- is normally not favorable, ionized paraformal-

198 dehyde-type hemiacetals are stabilized by interactions between the ionized —O^- and
199 the other terminal hydroxyl group(s) on the molecule (see the Supporting Infor-
200 mation).

201 The peaks at m/z 176.7 and 193.8 amu are not observed in the formaldehyde- H_2O
202 spectrum, implying that the species observed at those masses are formed via reaction
203 with AS. Within our instrument resolution, these peaks could be consistent with
204 methanol, which is present in our system due to its use as a stabilizer in formaldehyde
205 solutions. However, methanol does not form stable clusters with Γ^- and therefore will
206 not be detected using this ionization scheme. The peak at 193.8 amu is consistent with
207 an organosulfate species formed from a formaldehyde hemiacetal dimer ($\text{C}_2\text{H}_5\text{O}_6\text{S}^-$
208 $\cdot 2\text{H}_2\text{O}$) and a satellite peak is also visible at 195.6 amu (see Supporting Information).
209 The abundance of these peaks should be consistent with a 96:4 ratio of stable sulfate
210 isotopes (^{32}S and ^{34}S), and instead this ratio is found to be 86:14. This is not incon-
211 sistent with the identification of an organosulfate species at 193.8 amu, but additional
212 compounds could also be present at 195.6 amu. The peak at 176.7 amu matches an ion
213 formula of $\text{C}_6\text{H}_9\text{O}_6^-$, but the structure and formation mechanism is unknown. Future
214 mechanistic studies are needed in order to resolve products such as this one with un-
215 known chemical structures and/or formation mechanisms.

216 The positive-ion spectrum of the formaldehyde solution in 3.1 M AS corroborates
217 the identification of hemiacetal oligomers. The formaldehyde hemiacetal dimer sul-
218 fate was not observed in positive-ion mode. This was expected, since, to our
219 knowledge, organosulfate species have not previously been observed using positive-
220 ion-mode mass spectrometry (Sareen et al., 2010). The spectrum and peak assign-
221 ments can be found in the Supporting Information.

222 **3.2.2 Formaldehyde-methylglyoxal mixtures.** The negative-ion spectrum (de-
223 tected with Γ^-) for an aqueous mixture of formaldehyde, MG, and AS is shown in Fig.
224 6, with peak assignments listed in Table 3. Most of the peaks are consistent with for-
225 maldehyde hemiacetal oligomers, such as 186.7, 203.5, 230.3, 257.4, and 264.5 amu.
226 Formic acid was detected at 172.8 amu and 208.7 amu. The peak at 288.1 corresponds

227 to MG self-reaction products formed either via aldol condensation or hemiacetal
228 mechanisms (Sareen et al., 2010; Schwier et al., 2010). Several peaks could corre-
229 spond to self-reaction products of either formaldehyde or MG: 216.5, 252.4, 324.5,
230 and 342.6 amu. The peak at 314.3 amu is consistent with a hemiacetal oligomer
231 formed via cross-reaction of MG with two formaldehyde molecules, clustered with I⁻
232 and two water molecules. The peak at 272.2 amu could correspond to either a similar
233 cross-reaction product (MG + 2 formaldehyde) or a MG dimer. Formaldehyde hemi-
234 acetal self-reaction products and formic acid were detected in the positive-ion spec-
235 trum (Supporting Information).

236 While the negative-ion spectra of the formaldehyde-AS and formaldehyde-MG-
237 AS mixtures share many similar peaks, there are some differences in the spectra.
238 Small variations in pressure and flow rates within the declustering region can affect
239 the clustering efficiency between the analyte and the parent ions, and surrounding wa-
240 ter molecules, resulting in the same analyte compound appearing at different m/z val-
241 ues.

242 **3.2.3 Acetaldehyde-methylglyoxal mixtures.** The $\text{H}_3\text{O}^+(\text{H}_2\text{O})_n$ spectrum for
243 aqueous acetaldehyde-MG-AS mixtures is shown in Figure 7, with peak assignments
244 listed in Table 4. Several peaks, specifically acetaldehyde aldol condensation products
245 (i.e. 88.9, 107.2, 192.9, 289.6, and 297 amu), are similar to those expected in acetal-
246 dehyde-AS solutions (Casale et al., 2007; Noziere et al., 2010a). Hydrated acetalde-
247 hyde can be observed at 98.4 amu. Several peaks are consistent with the cross-
248 reaction products of MG and acetaldehyde via an aldol mechanism (126.0, 134.0,
249 206.7, and 248.9 amu). Formic, glyoxylic, and glycolic acids correspond to the peaks
250 at 84.4, 93.5, and 95.5 amu, respectively. A trace amount of formic acid impurity ex-
251 ists in the 37% formaldehyde aqueous stock solution. Since no significant source of
252 oxidants exists in the reaction mixtures, the formation mechanisms for these species
253 in this system are unknown. The peaks at 88.9 and 107.2 are consistent with either
254 pyruvic acid or crotonaldehyde. Large aldol condensation products from the addition
255 of 6-10 acetaldehydes are observed at 192.9, 289.6, and 297 amu. The peaks at 145.1,

256 162.9, 164.7 and 235 amu are consistent with MG self-reactions, as discussed by Sa-
257 reen et al (2010). The peak at 137.3 amu is consistent with a species with molecular
258 formula $C_5H_{12}O_3$, but the mechanism is unknown.

259 The I^- negative-ion spectrum for acetaldehyde-MG-AS mixtures shows similar
260 results to the positive-ion spectrum (see Figure 8 and Table 5), however aldol conden-
261 sation products are not detected by this method unless they contain a terminal carbox-
262 ylic acid group or neighboring hydroxyl groups (Sareen et al., 2010). Small acid spe-
263 cies, such as formic, acetic and crotonic acid (172.7 (208.4), 186.4 and 230.7 amu,
264 respectively), were detected. Hydrated acetaldehyde (189.6 and 224.1 amu) and MG
265 (216.3 amu), and hemiacetal self-dimers of acetaldehyde and MG (230.7, 256.4,
266 264.4, 269.5, and 342.3) were also observed. 256.4 amu is consistent with a MG aldol
267 condensation dimer product, and 272.2 amu could correspond either to a MG hemiac-
268 etal dimer or an aldol condensation product. 242.9 amu, $I^- \cdot C_5H_8O_3$, is consistent with
269 an aldol condensation cross product of MG and acetaldehyde. 194.6 amu corresponds
270 to $C_6H_9O_6^-$ (mechanism and structure unknown).

271 Note that several peaks appear at similar mass-to-charge ratios in the negative
272 mode mass spectra of both the formaldehyde-MG and acetaldehyde-MG mixtures.
273 MG self-reaction products are expected to be present in both systems. Beyond this,
274 formaldehyde and acetaldehyde are structurally similar small molecules which follow
275 similar oligomerization mechanisms alone and with MG. In several cases, peaks in the
276 mass spectra corresponding to structurally distinct expected reaction products for each
277 system have similar mass-to-charge ratios. For example, the formaldehyde hemiacetal
278 4-mer ($I^- \cdot C_4H_{10}O_5$) and the acetaldehyde dimer ($I^- \cdot C_4H_6O_3 \cdot 2H_2O$) are both apparent at
279 264 amu.

280 **4. Discussion**

281 Both formaldehyde and acetaldehyde, and their aqueous-phase reaction products,
282 were found to depress surface tension in AS solutions. However, surface tension de-
283 pression was not observed in aqueous formaldehyde solutions containing no salt, due

284 to the hydrophilic character of hydrated formaldehyde and its oligomer products. Net
285 surface tension depression by acetaldehyde was greater in the AS solutions than in
286 pure water. These differences for both organics are likely due to chemical and physi-
287 cal effects of “salting out” (Setschenow, 1889), which may enhance organic film for-
288 mation on the surface of a pendant drop (or aerosol particle). The salt promotes the
289 formation of surface-active species: several of the reaction products in the AS systems
290 identified using Aerosol-CIMS are known or expected to be surface-active, such as
291 organosulfates (Noziere et al., 2010b) and organic acids. Salts can also alter the parti-
292 tioning of these volatile yet water-soluble organic species between the gas phase and
293 aqueous solution. Formaldehyde has a small Henry’s Law constant of 2.5 M atm^{-1} ,
294 although hydration in the aqueous phase leads to an effective Henry’s Law constant of
295 $3 \times 10^3 \text{ M atm}^{-1}$, similar to that of MG (Betterton and Hoffmann, 1988; Seinfeld and
296 Pandis, 1998). The effective Henry’s Law constant for acetaldehyde in water at 25°C
297 was measured by Betterton and Hoffmann (1988) to be 11.4 M atm^{-1} . The Henry’s
298 Law constant of formaldehyde was shown by Zhou and Mopper to increase slightly in
299 aqueous solutions containing an increasing proportion of seawater (up to 100%), but
300 the opposite is true for acetaldehyde (Zhou and Mopper, 1990). The reaction mixtures
301 studied here equilibrated with the headspace of the closed container for 24 h before
302 the surface tension measurements were performed. Each pendant drop equilibrated for
303 2 min before image capture, after which time there was no detectable change in drop
304 shape. Some of the organics may be lost to the gas phase during equilibration. How-
305 ever, the lower volatility of the aqueous-phase reaction products, especially those
306 formed through oligomerization, leads to significant organic material remaining in the
307 condensed phase (enough to cause surface tension depression and be detected via
308 Aerosol-CIMS).

309 When formaldehyde and acetaldehyde are present in combination with MG, as
310 would likely happen in the atmosphere (Fung and Wright, 1990; Grosjean, 1982;
311 Munger et al., 1995), there is a synergistic effect: surface tension depression in the
312 solutions containing mixed organics exceeds that predicted by an additive model

313 based on the single-species isotherms. This effect could be due to the formation of
314 more surface-active reaction products in the mixed systems. The deviation from the
315 Henning model prediction was less than 10% except in the case of the acetaldehyde-
316 MG-AS mixtures. Between 21-30% of the detected product mass was identified as
317 cross products in the Aerosol-CIMS positive mode analysis of the acetaldehyde-MG
318 mixtures following (Schwier et al., 2010). Most of the oligomers identified in this sys-
319 tem were aldol condensation products, which have fewer hydroxyl groups than acetal
320 oligomers and are therefore expected to be more hydrophobic. A number of organic
321 acid products, likely to be surface-active, were also identified in the acetaldehyde-
322 MG-AS system.

323 In contrast to the MG-glyoxal system, the presence of formaldehyde and/or acet-
324 aldehyde in aqueous MG-AS solutions does influence surface tension depression, in
325 fact, to a greater extent than predicted by the Henning model. However, the results of
326 the binary and ternary mixture experiments suggest that MG still plays a dominant
327 role in these systems since the measured surface tension was remarkably similar in
328 each mixture for a given MG concentration.

329 The formaldehyde hemiacetal dimer sulfate ($C_2H_6O_6S$) may form via the reaction
330 of $C_2H_6O_3$ with H_2SO_4 (Deno and Newman, 1950) (see the Supporting Information
331 for detailed discussion and calculations). The equilibrium concentration of H_2SO_4 in
332 our bulk solutions (3.1 M AS, pH = 3) is small (2.8×10^{-7} M). Minerath and coworkers
333 showed that alcohol sulfate ester formation is slow under tropospheric aerosol condi-
334 tions (Minerath et al., 2008). Based on our observations, assuming a maximum Aero-
335 sol-CIMS sensitivity of 100 Hz ppt⁻¹ to this species (Sareen et al., 2010) we infer a
336 concentration of $\geq 2 \times 10^{-4}$ M in the bulk solution after 24 h of reaction. Using our ex-
337 perimental conditions and the kinetics of ethylene glycol sulfate esterification from
338 Minerath et al., we predict a maximum concentration of 7×10^{-8} M. This disagreement
339 between model and experiment suggests that either a) the kinetics of sulfate esterifica-
340 tion for paraformaldehyde are significantly faster than for alcohols b) SO_4^{-2} or HSO_4^-
341 is the active reactant, contrary to the conclusions of Deno and Newman, or c) sulfate

342 esterification is enhanced by the solution dehydration that accompanies the atomization and
343 volatilization steps in our detection technique. Photochemical production of organosul-
344 fates has also been observed (Galloway et al., 2009; Noziere et al., 2010b; Perri et al.,
345 2010). Our samples were protected from UV light by the Pyrex reaction vessels, and
346 no significant OH source was present, so we don't expect photochemical organosul-
347 fate production to be efficient in this system.

348 Nitrogen-containing compounds could also be formed in these reaction mixtures
349 due to the presence of the ammonium ion (Galloway et al., 2009; Noziere et al., 2009;
350 Sareen et al., 2010). No unambiguous identifications of C-N containing products were
351 made in this study, but analysis using a mass spectrometry technique with higher mass
352 resolution could reveal their presence.

353 Ambient aerosol concentrations of formaldehyde and acetaldehyde have been
354 measured up to $0.26 \mu\text{g m}^{-3}$ formaldehyde and $0.4 \mu\text{g m}^{-3}$ acetaldehyde in Los Ange-
355 les (Grosjean, 1982). Using a dry aerosol mass of $50 \mu\text{g m}^{-3}$, at a relative humidity of
356 80% (with a mass ratio of water:solute of 1), these ambient in-particle concentrations
357 of formaldehyde and acetaldehyde correspond to 0.17 and 0.18 mol/kg H_2O , respec-
358 tively, which are within the concentration ranges used in this study. At these realistic
359 concentrations, we observed non-negligible surface tension depression by formalde-
360 hyde and acetaldehyde (8.8% and 12.1%, respectively). However, if we assume a rela-
361 tive humidity of 99%, relevant for cloud droplet activation, the mass ratio of wa-
362 ter:solute increases to 35, so the in-particle concentrations correspond to 0.0049 and
363 0.0052 mol/kg H_2O , respectively, which is below the concentration ranges used. Rela-
364 tively high aldehyde concentrations are considered justified to mimic the aerosol
365 phase in experiments, which was our intent here (Ervens et al., 2011; Sareen et al.,
366 2010; Tan et al., 2009; Tan et al., 2010). Furthermore, the extended concentration
367 range used here was chosen to enable us to characterize the surface tension behavior
368 using the Szyszkowski-Langmuir equation.

369 The relatively small Henry's Law partitioning of formaldehyde and acetaldehyde
370 to water suggests that their potential to contribute to total SOA mass is low as com-

371 pared to highly soluble species such as glyoxal. This is supported by the observations
372 of Kroll et al. (2005) that AS aerosols exposed to formaldehyde in an aerosol reaction
373 chamber did not result in significant particle volume growth. However, recent studies
374 have indicated that aldehydes partition into the aqueous particle phase more than pre-
375 dicted by Henry's Law (Baboukas et al., 2000; Grosjean, 1982; Healy et al., 2008);
376 this is hypothesized to be a hydration equilibrium shift (Yu et al., 2011). Grosjean et
377 al. determined that in-particle concentrations were up to 3 orders of magnitude higher
378 for formaldehyde than those predicted by Henry's Law (using an aerosol mass $150 \mu\text{g}$
379 m^{-3} and 15% water content). Additionally, formaldehyde and acetaldehyde in the gas
380 phase could adsorb at the aerosol surface (vs. bulk aqueous absorption), and this may
381 also impact aerosol surface tension (Donaldson and Vaida, 2006). Furthermore,
382 Romakkaniemi and coworkers recently showed significant enhancement of aqueous-
383 phase SOA production by surface-active species when OH oxidation is also occurring,
384 beyond what would be predicted based on Henry's Law due to surface-bulk partition-
385 ing (Romakkaniemi et al., 2011).

386 **5. Conclusions**

387 Two highly volatile organic compounds, formaldehyde and acetaldehyde, were found
388 to form secondary organic products in aqueous ammonium sulfate (AS) solutions
389 mimicking tropospheric aerosols. These species, and their aqueous-phase reaction
390 products, lead to depressed surface tension in the aqueous solutions. This adds to the
391 growing body of evidence that VOCs are a secondary source of surface-active organic
392 material in aerosols.

393

394 **Acknowledgement**

395 This work was funded by the NASA Tropospheric Chemistry program (grant
396 NNX09AF26G) and the ACS Petroleum Research Fund (Grant 48788-DN14). The

397 authors gratefully acknowledge the Koberstein group at Columbia University for use
398 of the pendant drop tensiometer.

399

400 **References**

- 401 Adamson, A. W. and Gast, A. P., Physical chemistry of surfaces, Wiley, New York,
402 1997.
- 403 Baboukas, E. D., Kanakidou, M., and Mihalopoulos, N.: Carboxylic acids in gas and
404 particulate phase above the Atlantic Ocean, *J. Geophys. Res.*, *105* (D11),
405 14459-14471, 2000.
- 406 Betterton, E. A. and Hoffmann, M. R.: Henry Law Constants of Some Environmental-
407 ly Important Aldehydes, *Environ. Sci. Technol.*, *22* (12), 1415-1418, 1988.
- 408 Casale, M. T., Richman, A. R., Elrod, M. J., Garland, R. M., Beaver, M. R., and Tol-
409 bert, M. A.: Kinetics of acid-catalyzed aldol condensation reactions of aliphatic
410 aldehydes, *Atmospheric Environment*, *41* (29), 6212-6224, 2007.
- 411 Deno, N. C. and Newman, M. S.: Mechanism of Sulfation of Alcohols, *Journal of the*
412 *American Chemical Society*, *72* (9), 3852-3856, 1950.
- 413 Djikaev, Y. S. and Tabazadeh, A.: Effect of adsorption on the uptake of organic trace
414 gas by cloud droplets, *Journal of Geophysical Research-Atmospheres*, *108*
415 (D22), 4869-doi:10.1029/2003JD003741, 2003.
- 416 Donaldson, D. J. and Vaida, V.: The influence of organic films at the air-aqueous
417 boundary on atmospheric processes, *Chemical Reviews*, *106* (4), 1445-1461,
418 2006.
- 419 Ervens, B., Turpin, B. J., and Weber, R. J.: Secondary organic aerosol formation in
420 cloud droplets and aqueous particles (aqSOA): a review of laboratory, field
421 and model studies, *Atmos. Chem. Phys. Discuss.*, *11* (8), 22301-22383, 2011.
- 422 Ervens, B. and Volkamer, R.: Glyoxal processing by aerosol multiphase chemistry:
423 Towards a kinetic modeling framework of secondary organic aerosol for-
424 mation in aqueous particles, *Atmos. Chem. Phys.*, *10* (8), 8219-8244, 2010.
- 425 Facchini, M. C., Mircea, M., Fuzzi, S., and Charlson, R. J.: Cloud albedo enhance-
426 ment by surface-active organic solutes in growing droplets, *Nature*, *401*
427 (6750), 257-259, 1999.
- 428 Folkers, M., Mentel, T. F., and Wahner, A.: Influence of an organic coating on the re-
429 activity of aqueous aerosols probed by the heterogeneous hydrolysis of N₂O₅,
430 *Geophysical Research Letters*, *30* (12), 1644-1647, 2003.

- 431 Fung, K. and Wright, B.: Measurement of Formaldehyde and Acetaldehyde using 2,4-
432 dinitrophenylhydrazine-impregnated cartridges during the carbonaceous spe-
433 cies methods comparison study, *Aerosol Science and Technology*, 12 (1), 44-
434 48, 1990.
- 435 Galloway, M. M., Chhabra, P. S., Chan, A. W. H., Surratt, J. D., Flagan, R. C., Sein-
436 feld, J. H., and Keutsch, F. N.: Glyoxal uptake on ammonium sulphate seed
437 aerosol: reaction products and reversibility of uptake under dark and irradiated
438 conditions, *Atmos.Chem.Phys.*, 9 (3331-3345, 2009.
- 439 Grosjean, D.: Formaldehyde and other carbonyl in Los Angeles ambient air, *Envi-
440 ron.Sci.Technol.*, 16 (5), 254-262, 1982.
- 441 Healy, R. M., Wenger, J. C., Metzger, A., Duplissy, J., Kalberer, M., and Dommen, J.:
442 Gas/particle partitioning of carbonyls in the photooxidation of isoprene and
443 1,3,5-trimethylbenzene, *Atmos.Chem.Phys.*, 8 (12), 3215-3230, 2008.
- 444 Henning, S., Rosenorn, T., D'Anna, B., Gola, A. A., Svenningsson, B., and Bilde, M.:
445 Cloud droplet activation and surface tension of mixtures of slightly soluble or-
446 ganics and inorganic salt, *Atmospheric Chemistry and Physics*, 5 (575-582,
447 2005.
- 448 Jimenez, J. L., Canagaratna, M. R., Donahue, N. M., Prevot, A. S. H., Zhang, Q.,
449 Kroll, J. H., DeCarlo, P. F., Allan, J. D., Coe, H., Ng, N. L., Aiken, A. C., Do-
450 cherty, K. S., Ulbrich, I. M., Grieshop, A. P., Robinson, A. L., Duplissy, J.,
451 Smith, J. D., Wilson, K. R., Lanz, V. A., Hueglin, C., Sun, Y. L., Tian, J.,
452 Laaksonen, A., Raatikainen, T., Rautiainen, J., Vaattovaara, P., Ehn, M.,
453 Kulmala, M., Tomlinson, J. M., Collins, D. R., Cubison, M. J., Dunlea, E. J.,
454 Huffman, J. A., Onasch, T. B., Alfarra, M. R., Williams, P. I., Bower, K., Kon-
455 do, Y., Schneider, J., Drewnick, F., Borrmann, S., Weimer, S., Demerjian, K.,
456 Salcedo, D., Cottrell, L., Griffin, R., Takami, A., Miyoshi, T., Hatakeyama, S.,
457 Shimono, A., Sun, J. Y., Zhang, Y. M., Dzepina, K., Kimmel, J. R., Sueper, D.,
458 Jayne, J. T., Herndon, S. C., Trimborn, A. M., Williams, L. R., Wood, E. C.,
459 Middlebrook, A. M., Kolb, C. E., Baltensperger, U., and Worsnop, D. R.: Evo-
460 lution of Organic Aerosols in the Atmosphere, *Science*, 326 (5959), 1525-
461 1529, 2009.
- 462 Kanakidou, M., Seinfeld, J. H., Pandis, S. N., Barnes, I., Dentener, F. J., Facchini, M.
463 C., Van Dingenen, R., Ervens, B., Nenes, A., Nielsen, C. J., Swietlicki, E., Pu-
464 taud, J. P., Balkanski, Y., Fuzzi, S., Horth, J., Moortgat, G. K., Winterhalter,
465 R., Myhre, C. E. L., Tsigaridis, K., Vignati, E., Stephanou, E. G., and Wilson,
466 J.: Organic aerosol and global climate modelling: a review, *Atmospheric
467 Chemistry and Physics*, 5, 1053-1123, 2005.
- 468 Kohler, H.: The nucleus in the growth of hygroscopic droplets, *Trans.Faraday Soc.*,
469 32, 1152-1161, 1936.

- 470 Lim, Y. B., Tan, Y., Perri, M. J., Seitzinger, S. P., and Turpin, B. J.: Aqueous chemistry
471 and its role in secondary organic aerosol (SOA) formation, *Atmospheric*
472 *Chemistry and Physics*, 10 (21), 10521-10539, 2010.
- 473 Loudon, G. M., Organic chemistry, Roberts and Co, Greenwood Village, Colo, 2009.
- 474 McNeill, V. F., Patterson, J., Wolfe, G. M., and Thornton, J. A.: The effect of varying
475 levels of surfactant on the reactive uptake of N₂O₅ to aqueous aerosol, *At-*
476 *mospheric Chemistry and Physics*, 6, 1635-1644, 2006.
- 477 Minerath, E. C., Casale, M. T., and Elrod, M. J.: Kinetics feasibility study of alcohol
478 sulfate esterification reactions in tropospheric aerosols, *Environ.Sci.Technol.*,
479 42 (12), 4410-4415, 2008.
- 480 Munger, J. W., Jacob, D. J., Daube, B. C., Horowitz, L. W., Keene, W. C., and Heikes,
481 B. G.: Formaldehyde, glyoxal, and methylglyoxal in air and cloudwater at a
482 rural mountain site in central Virginia, *Journal of Geophysical Research*, 100
483 (D5), 9325-9333, 1995.
- 484 Noziere, B., Dziedzic, P., and Cordova, A.: Products and Kinetics of the Liquid-Phase
485 Reaction of Glyoxal Catalyzed by Ammonium Ions (NH₄⁺), *Journal of Physi-*
486 *cal Chemistry A*, 113 (1), 231-237, 2009.
- 487 Noziere, B., Dziedzic, P., and Cordova, A.: Inorganic ammonium salts and carbonate
488 salts are efficient catalysts for aldol condensation in atmospheric aerosols,
489 *Physical Chemistry Chemical Physics*, 12 (15), 3864-3872, 2010a.
- 490 Noziere, B., Ekstrom, S., Alsberg, T., and Holmstrom, S.: Radical-initiated formation
491 of organosulfates and surfactants in atmospheric aerosols, *Geophysical Re-*
492 *search Letters*, 37, L05806, doi:10.1029/2009GL041683, 2010b.
- 493 Perri, M. J., Lim, Y. B., Seitzinger, S. P., and Turpin, B. J.: Organosulfates from gly-
494 colaldehyde in aqueous aerosols and clouds: Laboratory studies, *Atmospheric*
495 *Environment*, 44 (21-22), 2658-2664, 2010.
- 496 Romakkaniemi, S., Kokkola, H., Smith, J. N., Prisle, N. L., Schwier, A. N., McNeill,
497 V. F., and Laaksonen, A.: Partitioning of Semivolatile Surface-Active Com-
498 pounds Between Bulk, Surface, and Gas-Phase, *Geophys.Res.Lett.*, 38 (3),
499 L03807, doi:10.1029/2010GL046147, 2011.
- 500 Sareen, N., Schwier, A. N., Shapiro, E. L., Mitroo, D. M., and McNeill, V. F.: Second-
501 ary organic material formed by methylglyoxal in aqueous aerosol mimics, *At-*
502 *mos.Chem.Phys.*, 10, 997-1016, 2010.
- 503 Schwier, A. N., Sareen, N., Mitroo, D. M., Shapiro, E. L., and McNeill, V. F.: Glyox-
504 al-Methylglyoxal Cross-Reactions in Secondary Organic Aerosol Formation,
505 *Environ.Sci.Technol.*, 44 (16), 6174-6182, 2010.

- 506 Seinfeld, J. H. and Pandis, S. N., Atmospheric chemistry and physics
507 from air pollution to climate change, Wiley, New York, 1998.
- 508 Setschenow, J. Z.: Uber Die Konstitution Der Salzosungen auf Grund ihres Verhaltens
509 zu Kohlensaure, *Z.Physik.Chem.*, 4, 117-125, 1889.
- 510 Shapiro, E. L., Szprengiel, J., Sareen, N., Jen, C. N., Giordano, M. R., and McNeill, V.
511 F.: Light-absorbing secondary organic material formed by glyoxal in aqueous
512 aerosol mimics, *Atmospheric Chemistry and Physics*, 9 (7), 2289-2300, 2009.
- 513 Shulman, M. L., Jacobson, M. C., Carlson, R. J., Synovec, R. E., and Young, T. E.:
514 Dissolution behavior and surface tension effects of organic compounds in nu-
515 cleating cloud droplets, *Geophysical Research Letters*, 23 (3), 277-280, 1996.
- 516 Tan, Y., Carlton, A. G., Seitzinger, S. P., and Turpin, B. J.: SOA from methylglyoxal in
517 clouds and wet aerosols: Measurement and prediction of key products, *At-
518 mos.Environ.*, 44 (39), 5218-5226, 2010.
- 519 Tan, Y., Perri, M. J., Seitzinger, S. P., and Turpin, B. J.: Effects of Precursor Concen-
520 tration and Acidic Sulfate in Aqueous Glyoxal-OH Radical Oxidation and Im-
521 plications for Secondary Organic Aerosol, *Environ.Sci.Technol.*, 43 (21),
522 8105-8112, 2009.
- 523 Wang, X. F., Gao, S., Yang, X., Chen, H., Chen, J. M., Zhuang, G. S., Surratt, J. D.,
524 Chan, M. N., and Seinfeld, J. H.: Evidence for High Molecular Weight Nitro-
525 gen-Containing Organic Salts in Urban Aerosols, *Environ.Sci.Technol.*, 44
526 (12), 4441-4446, 2010.
- 527 Yu, G., Bayer, A. R., Galloway, M. M., Korshavn, K. J., Fry, C. G., and Keutsch, F.
528 N.: Glyoxal in Aqueous Ammonium Sulfate Solutions: Products, Kinetics and
529 Hydration Effects, *Environ.Sci.Technol.*, 45 (15), 6336-6342, 2011.
- 530 Zhou, X. L. and Mopper, K.: Apparent Partition-Coefficients of 15 Carbonyl-
531 Compounds Between Air and Seawater and Between Air and Fresh-Water -
532 Implications for Air Sea Exchange, *Environ.Sci.Technol.*, 24 (12), 1864-1869,
533 1990.
534
535

536 **Table 1.** Szyszkowski-Langmuir Fit Parameters according to Eq. (2)

Mixture	σ_0 (dyn cm ⁻¹)	a (dyn cm ⁻¹ K ⁻¹)	b (kg H ₂ O (mol C) ⁻¹)
Methylglyoxal + 3.1 M (NH ₄) ₂ SO ₄ (Sareen et al. 2010)	78.5	0.0185±0.0008	140±34
Acetaldehyde + 3.1 M (NH ₄) ₂ SO ₄	78.5	0.0008±0.0046	9.53±3.86
Formaldehyde + 3.1 M (NH ₄) ₂ SO ₄	78.5	0.0119±0.0043	50.23±44.8
Acetaldehyde + H ₂ O	72.0	0.0037±0.0011	491.64±689

537

538

539 **Table 2.** Proposed peak assignments for Aerosol-CIMS mass spectra with Γ^- of atom-
540 ized solutions of 0.2 M formaldehyde in 3.1 M AS.

m/z (amu) ± 1.0 amu	Ion Formula	Molecular Formula	Possible Structures	Mechanism
81.7	CHO ₂ ⁻ ·2H ₂ O	CH ₂ O ₂		Formic Acid
95.6	C ₂ H ₅ O ₃ ⁻ ·H ₂ O	C ₂ H ₆ O ₃		n=2 hemiacetal
110.4	C ₂ H ₃ O ₃ ⁻ ·2H ₂ O	C ₂ H ₄ O ₃		n=2 hemiacetal
176.7	C ₆ H ₉ O ₆ ⁻	C ₆ H ₁₀ O ₆	Unknown	Unknown
193.8	C ₂ H ₅ O ₆ S ⁻ ·2H ₂ O	C ₂ H ₆ O ₆ S		Hemiacetal sulfate
208.7	Γ^- ·CH ₂ O ₂ ·2H ₂ O	CH ₂ O ₂		Formic Acid
223.3	Γ^- ·C ₂ H ₆ O ₃ ·H ₂ O	C ₂ H ₆ O ₃		n=2 hemiacetal
273.8	C ₈ H ₁₅ O ₉ ⁻ ·H ₂ O C ₈ H ₁₇ O ₁₀ ⁻	C ₈ H ₁₆ O ₉ C ₈ H ₁₈ O ₁₀		n=8 hemiacetal
291.1	Γ^- ·C ₅ H ₈ O ₆	C ₅ H ₈ O ₆		n=5 hemiacetal
304.7	C ₉ H ₁₉ O ₁₀ ⁻ ·H ₂ O	C ₉ H ₂₀ O ₁₀		n=9 hemiacetal
323.5	Γ^- ·C ₆ H ₁₄ O ₇	C ₆ H ₁₄ O ₇		n=6 hemiacetal

541

542 **Table 3.** Proposed peak assignments for Aerosol-CIMS mass spectra with I^- of atom-
543 ized solutions of 2 M formaldehyde/MG (1:1) in 3.1 M AS.

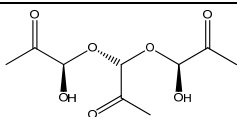
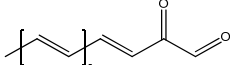
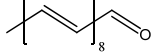
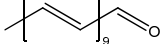
m/z (amu) ± 1.0 amu	Ion Formula	Molecular Formula	Possible Structures	Mechanism
172.8	$\text{I}^- \cdot \text{CH}_2\text{O}_2$	CH_2O_2		Formic Acid
186.7	$\text{I}^- \cdot \text{C}_2\text{H}_4\text{O}_2$	$\text{C}_2\text{H}_4\text{O}_2$		cyclic F acetal
203.5	$\text{C}_5\text{H}_{11}\text{O}_6^- \cdot 2\text{H}_2\text{O}$	$\text{C}_5\text{H}_{12}\text{O}_6$		n=5 F hemiacetal
208.7	$\text{I}^- \cdot \text{CH}_2\text{O}_2 \cdot 2\text{H}_2\text{O}$	CH_2O_2		Formic Acid
216.5	$\text{I}^- \cdot \text{C}_3\text{H}_6\text{O}_3$	$\text{C}_3\text{H}_6\text{O}_3$		Hydrated MG or cyclic F acetal
230.3	$\text{I}^- \cdot \text{C}_3\text{H}_4\text{O}_4$	$\text{C}_3\text{H}_4\text{O}_4$		n = 3 F hemiacetal
252.4	$\text{I}^- \cdot \text{C}_6\text{H}_6\text{O}_3$ $\text{I}^- \cdot \text{C}_3\text{H}_8\text{O}_4 \cdot \text{H}_2\text{O}$ $\text{I}^- \cdot \text{C}_3\text{H}_6\text{O}_3 \cdot 2\text{H}_2\text{O}$	$\text{C}_6\text{H}_6\text{O}_3$ $\text{C}_3\text{H}_8\text{O}_4$ $\text{C}_3\text{H}_6\text{O}_3$		MG aldol, n = 3 F hemiacetal, Hydrated MG, or cyclic F acetal
257.4	$\text{C}_8\text{H}_{17}\text{O}_9^-$	$\text{C}_8\text{H}_{18}\text{O}_9$		n=8 F hemiacetal
264.5	$\text{I}^- \cdot \text{C}_4\text{H}_{10}\text{O}_5$	$\text{C}_4\text{H}_{10}\text{O}_5$		n=4 F hemiacetal
272.2	$\text{I}^- \cdot \text{C}_6\text{H}_{10}\text{O}_4$	$\text{C}_6\text{H}_{10}\text{O}_4$		MG aldol and hemiacetal
	$\text{I}^- \cdot \text{C}_5\text{H}_6\text{O}_5$	$\text{C}_5\text{H}_6\text{O}_5$		MG + 2F hemiacetal
288.1	$\text{I}^- \cdot \text{C}_6\text{H}_{10}\text{O}_5$ $\text{I}^- \cdot \text{C}_6\text{H}_8\text{O}_4 \cdot \text{H}_2\text{O}$ $\text{I}^- \cdot \text{C}_6\text{H}_6\text{O}_3 \cdot 2\text{H}_2\text{O}$	$\text{C}_6\text{H}_{10}\text{O}_5$ $\text{C}_6\text{H}_8\text{O}_4$ $\text{C}_6\text{H}_6\text{O}_3$		MG aldol and hemiacetal
314.3	$\text{I}^- \cdot \text{C}_5\text{H}_{12}\text{O}_5 \cdot 2\text{H}_2\text{O}$	$\text{C}_5\text{H}_{12}\text{O}_5$		MG + 2F hemiacetal
324.5	$\text{I}^- \cdot \text{C}_6\text{H}_{14}\text{O}_7$ $\text{I}^- \cdot \text{C}_6\text{H}_{12}\text{O}_6 \cdot \text{H}_2\text{O}$ $\text{I}^- \cdot \text{C}_6\text{H}_{10}\text{O}_5 \cdot 2\text{H}_2\text{O}$	$\text{C}_6\text{H}_{14}\text{O}_7$ $\text{C}_6\text{H}_{12}\text{O}_6$ $\text{C}_6\text{H}_{10}\text{O}_5$		n=6 F hemiacetal, MG hemiacetal
342.6	$\text{I}^- \cdot \text{C}_6\text{H}_{14}\text{O}_7 \cdot \text{H}_2\text{O}$ $\text{I}^- \cdot \text{C}_6\text{H}_{12}\text{O}_6 \cdot 2\text{H}_2\text{O}$	$\text{C}_6\text{H}_{14}\text{O}_7$ $\text{C}_6\text{H}_{12}\text{O}_6$		n=6 F hemiacetal, MG hemiacetal

544
545

546
547

Table 4. Proposed peak assignments for Aerosol-CIMS mass spectra with H_3O^+ of atomized solutions of 0.5 M acetaldehyde/MG (1:1) in 3.1 M AS

m/z (amu) ± 1.0 amu	Ion Formula	Molecular Formula	Possible Structures	Mechanism
84.4	$\text{CH}_3\text{O}_2^+ \cdot 2\text{H}_2\text{O}$	CH_2O_2		Formic Acid
88.9	$\text{C}_3\text{H}_5\text{O}_3^+$	$\text{C}_3\text{H}_4\text{O}_3$		Pyruvic Acid
	$\text{C}_4\text{H}_7\text{O}^+ \cdot \text{H}_2\text{O}$ $\text{C}_4\text{H}_9\text{O}_2^+$	$\text{C}_4\text{H}_6\text{O}$ $\text{C}_4\text{H}_8\text{O}_2$		A aldol
93.5	$\text{C}_2\text{H}_3\text{O}_3^+ \cdot \text{H}_2\text{O}$	$\text{C}_2\text{H}_2\text{O}_3$		Glyoxylic Acid
95.5	$\text{C}_2\text{H}_5\text{O}_3^+ \cdot \text{H}_2\text{O}$	$\text{C}_2\text{H}_4\text{O}_3$		Glycolic Acid
98.4	$\text{C}_2\text{H}_7\text{O}_2^+ \cdot 2\text{H}_2\text{O}$	$\text{C}_2\text{H}_6\text{O}_2$		Hydrated A
107.2	$\text{C}_3\text{H}_5\text{O}_3^+ \cdot \text{H}_2\text{O}$	$\text{C}_3\text{H}_4\text{O}_3$		Pyruvic Acid
	$\text{C}_4\text{H}_9\text{O}_2^+ \cdot \text{H}_2\text{O}$	$\text{C}_4\text{H}_8\text{O}_2$		A aldol
126.0	$\text{C}_7\text{H}_9\text{O}_2^+$	$\text{C}_7\text{H}_8\text{O}_2$		MG + 2 A aldol
134.0	$\text{C}_5\text{H}_{11}\text{O}_4^+ \cdot \text{H}_2\text{O}$	$\text{C}_5\text{H}_{10}\text{O}_4$		MG + A aldol
137.3	$\text{C}_5\text{H}_{11}\text{O}_3^+ \cdot \text{H}_2\text{O}$	$\text{C}_5\text{H}_{10}\text{O}_3$		Unknown
145.1	$\text{C}_6\text{H}_9\text{O}_4^+$ $\text{C}_6\text{H}_7\text{O}_3^+ \cdot \text{H}_2\text{O}$	$\text{C}_6\text{H}_8\text{O}_4$ $\text{C}_6\text{H}_6\text{O}_3$		MG aldol
162.9	$\text{C}_6\text{H}_{11}\text{O}_5^+$ $\text{C}_6\text{H}_9\text{O}_4^+ \cdot \text{H}_2\text{O}$	$\text{C}_6\text{H}_{10}\text{O}_5$ $\text{C}_6\text{H}_8\text{O}_4$		MG hemiacetal and aldol
164.7	$\text{C}_6\text{H}_{13}\text{O}_5^+$	$\text{C}_6\text{H}_{12}\text{O}_5$		MG aldol
	$\text{C}_6\text{H}_{11}\text{O}_4^+ \cdot \text{H}_2\text{O}$	$\text{C}_6\text{H}_{10}\text{O}_4$		MG hemiacetal and aldol
192.9	$\text{C}_{12}\text{H}_{15}\text{O}^+ \cdot \text{H}_2\text{O}$	$\text{C}_{12}\text{H}_{14}\text{O}$		6 A aldol
206.7	$\text{C}_{11}\text{H}_{11}\text{O}_4^+$	$\text{C}_{11}\text{H}_{10}\text{O}_4$		A + 3 MG aldol

235	$C_9H_{15}O_7^+$	$C_9H_{14}O_7$		MG hemiacetal
248.9	$C_{15}H_{17}O_2^+ \cdot H_2O$	$C_{15}H_{16}O_2$		1MG + 6 A aldol
289.6	$C_{18}H_{21}O^+ \cdot 2H_2O$	$C_{18}H_{20}O$		9 A aldol
297	$C_{20}H_{23}O^+ \cdot H_2O$	$C_{20}H_{22}O$		10 A aldol

548

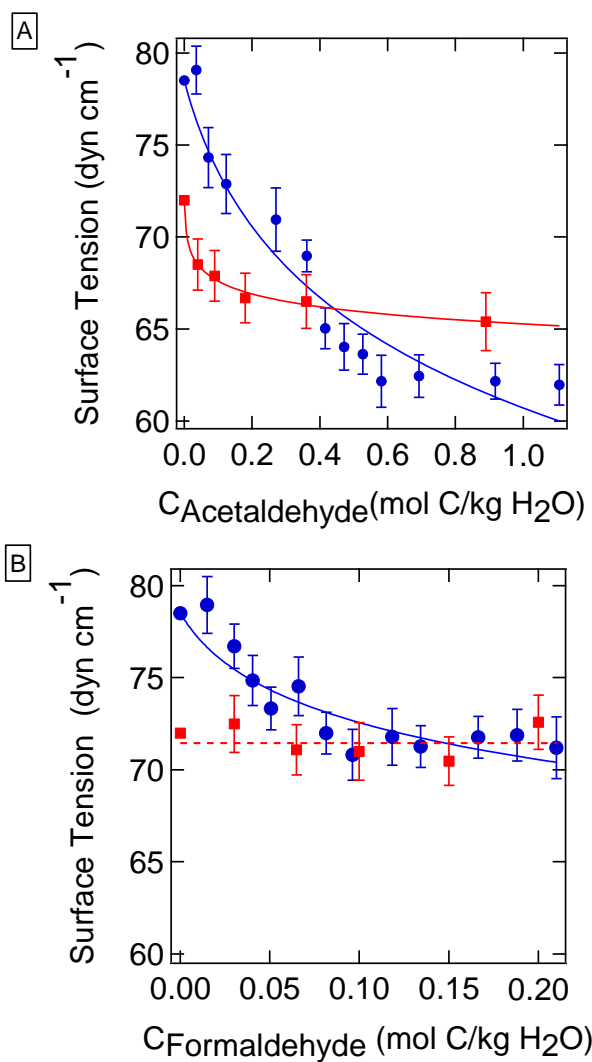
549

550
551

Table 5. Proposed peak assignments for Aerosol-CIMS mass spectra with Γ of atomized solutions of 2 M acetaldehyde/MG (1:1) in 3.1 M AS.

m/z (amu) \pm 1.0 amu	Ion Formula	Molecular Formula	Possible Structures	Mechanism
172.7	$\Gamma \cdot \text{CH}_2\text{O}_2$ $\Gamma \cdot \text{C}_2\text{H}_6\text{O}$	CH_2O_2 $\text{C}_2\text{H}_6\text{O}$		Formic Acid
186.4	$\Gamma \cdot \text{C}_2\text{H}_4\text{O}_2$	$\text{C}_2\text{H}_4\text{O}_2$		Acetic Acid
189.6	$\Gamma \cdot \text{C}_2\text{H}_6\text{O}_2$	$\text{C}_2\text{H}_6\text{O}_2$		Hydrated A
194.6	$\text{C}_6\text{H}_9\text{O}_6^-$ $\text{C}_2\text{H}_7\text{O}_6\text{S}^- \cdot \text{H}_2\text{O}$	$\text{C}_6\text{H}_{10}\text{O}_6$ $\text{C}_2\text{H}_8\text{O}_6\text{S}$	Unknown	Unknown
208.4	$\Gamma \cdot \text{CH}_2\text{O}_2 \cdot 2\text{H}_2\text{O}$	CH_2O_2		Formic Acid
216.3	$\Gamma \cdot \text{C}_3\text{H}_6\text{O}_3$	$\text{C}_3\text{H}_6\text{O}_3$		Hydrated MG
224.1	$\Gamma \cdot \text{C}_2\text{H}_6\text{O}_2 \cdot 2\text{H}_2\text{O}$	$\text{C}_2\text{H}_6\text{O}_2$		Hydrated A
230.7	$\Gamma \cdot \text{C}_4\text{H}_8\text{O}_3$	$\text{C}_4\text{H}_8\text{O}_3$		A hemiacetal
	$\Gamma \cdot \text{C}_4\text{H}_6\text{O}_2 \cdot \text{H}_2\text{O}$	$\text{C}_4\text{H}_6\text{O}_2$		Crotonic acid
242.9	$\Gamma \cdot \text{C}_5\text{H}_8\text{O}_3$	$\text{C}_5\text{H}_8\text{O}_3$		MG + A aldol
256.4	$\Gamma \cdot \text{C}_6\text{H}_{10}\text{O}_3$	$\text{C}_6\text{H}_{10}\text{O}_3$		MG aldol
264.4	$\Gamma \cdot \text{C}_4\text{H}_6\text{O}_3 \cdot 2\text{H}_2\text{O}$	$\text{C}_4\text{H}_6\text{O}_3$		A hemiacetal
269.5	$\Gamma \cdot \text{C}_4\text{H}_{10}\text{O}_3 \cdot 2\text{H}_2\text{O}$	$\text{C}_4\text{H}_{10}\text{O}_3$		A hemiacetal
272.2	$\Gamma \cdot \text{C}_6\text{H}_{10}\text{O}_4$	$\text{C}_6\text{H}_{10}\text{O}_4$		MG aldol and hemiacetal
342.3	$\Gamma \cdot \text{C}_6\text{H}_{12}\text{O}_6 \cdot 2\text{H}_2\text{O}$	$\text{C}_6\text{H}_{12}\text{O}_6$		MG hemiacetal

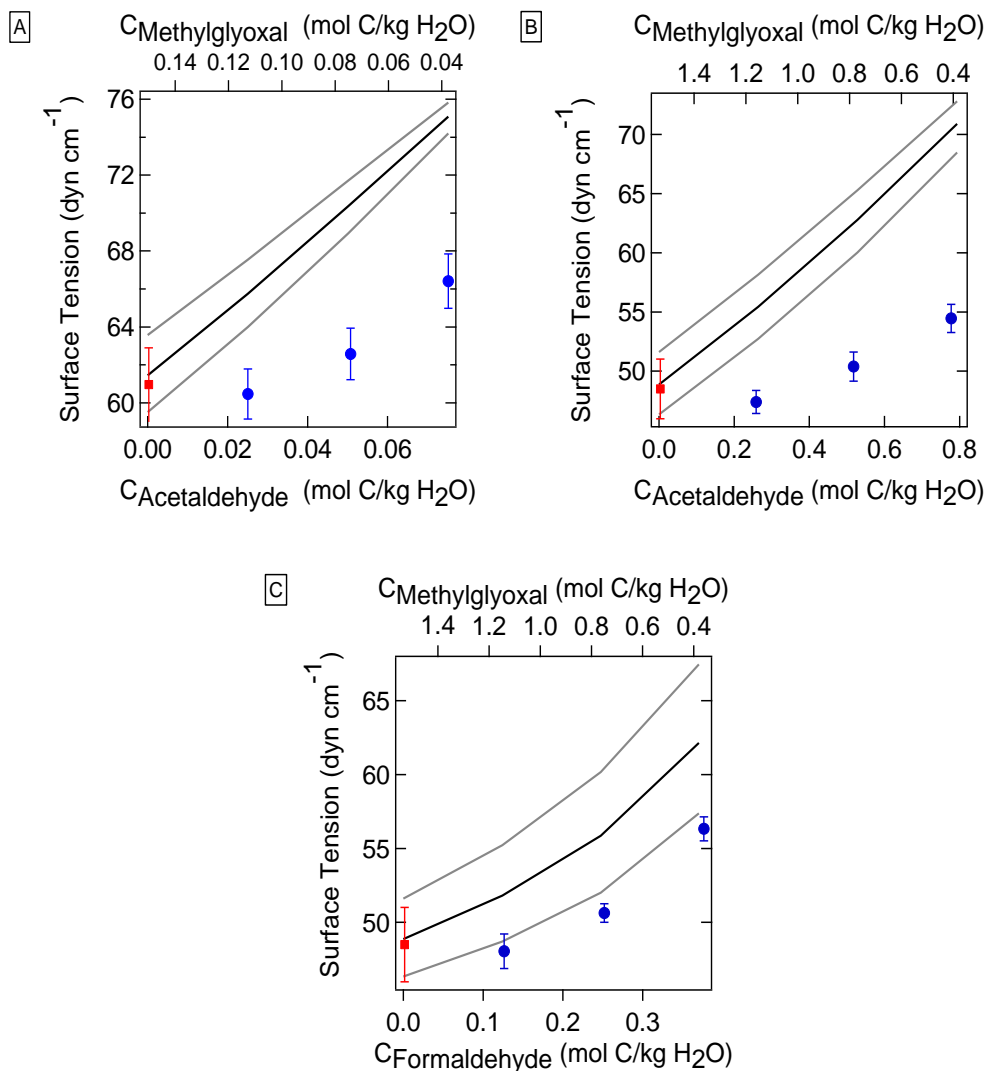
552
553



555

556 **Figure 1.** Surface tension of solutions containing (A) acetaldehyde and (B) formalde-
557 hyde in 3.1 M AS (●) and in water (■). The curves shown are fits to the data using the
558 Szyszkowski-Langmuir equation (Eq. (2)). A linear fit (red dashed line) is shown for
559 the formaldehyde-water data as a guide to the eye.

560

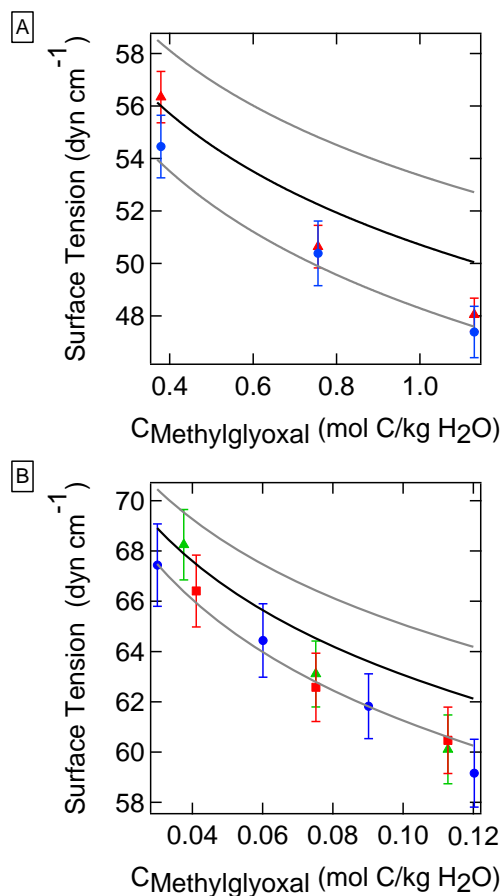


561

562

563 **Figure 2.** Surface tension of binary mixtures of acetaldehyde or formaldehyde with
 564 MG in 3.1 M AS solutions. The total organic concentration was 0.05 M (A) or 0.5 M
 565 (B, C). The black line shows Henning model predictions (Eq. (3)) using the parame-
 566 ters listed in Table 1. The grey lines show the confidence interval of the model predic-
 567 tions. ■: MG in AS (based on the Szyszkowski-Langmuir equation (Eq. (2)), using the
 568 parameters in Table 1). ●: Acetaldehyde (A and B) or Formaldehyde (C) with MG in
 569 3.1 M AS solutions.

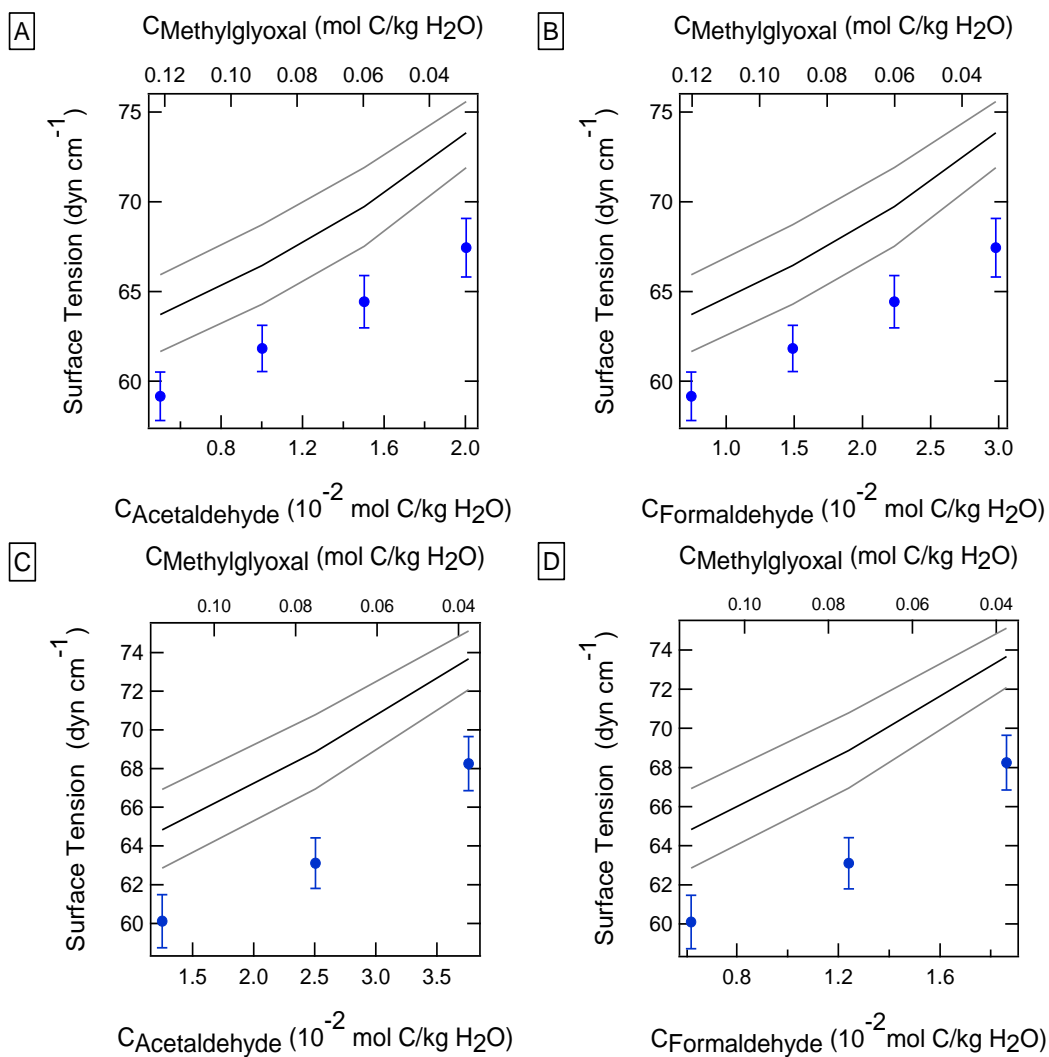
570



571

572 **Figure 3.** Surface tension in binary and ternary organic mixtures (Fig 2 & 3) as a
 573 function of MG concentration. A) Binary mixtures (0.5 M total organic concentration)
 574 ▲: acetaldehyde-MG, ●: formaldehyde-MG B) 0.05 M total organic concentration.
 575 ▲: ternary mixture (acetaldehyde:formaldehyde=1:1 by mole, varying MG); ●: ter-
 576 nary mixture (acetaldehyde:formaldehyde=1:3 by mole, varying MG); ■: binary mix-
 577 ture (acetaldehyde-MG). Black curves indicate the Szyszkowski-Langmuir curve for
 578 MG in AS using the parameters in Table 1. Grey curves show the confidence inter-
 579 vals.

580



581

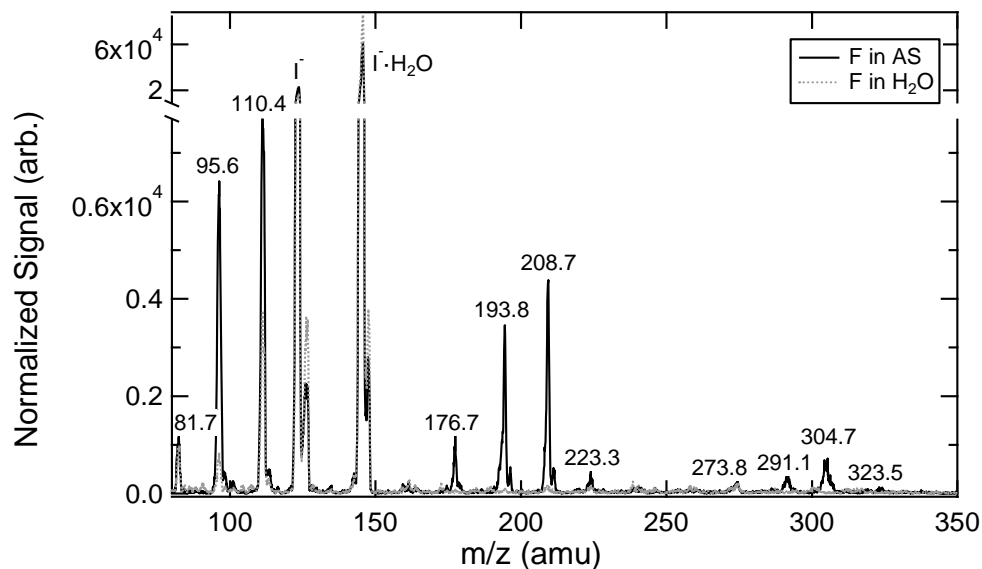
582 **Figure 4.** Surface tension data for ternary (acetaldehyde, formaldehyde and MG) mix-
 583 tures in 3.1 M AS solutions. The molar ratios of acetaldehyde to formaldehyde are 1:3
 584 (A and B) and 1:1 (C and D). The total organic concentration was constant at 0.05 M.
 585 The black line shows Henning model predictions using the parameters listed in Table
 586 1. The grey lines show the confidence interval of the predicted data.

587

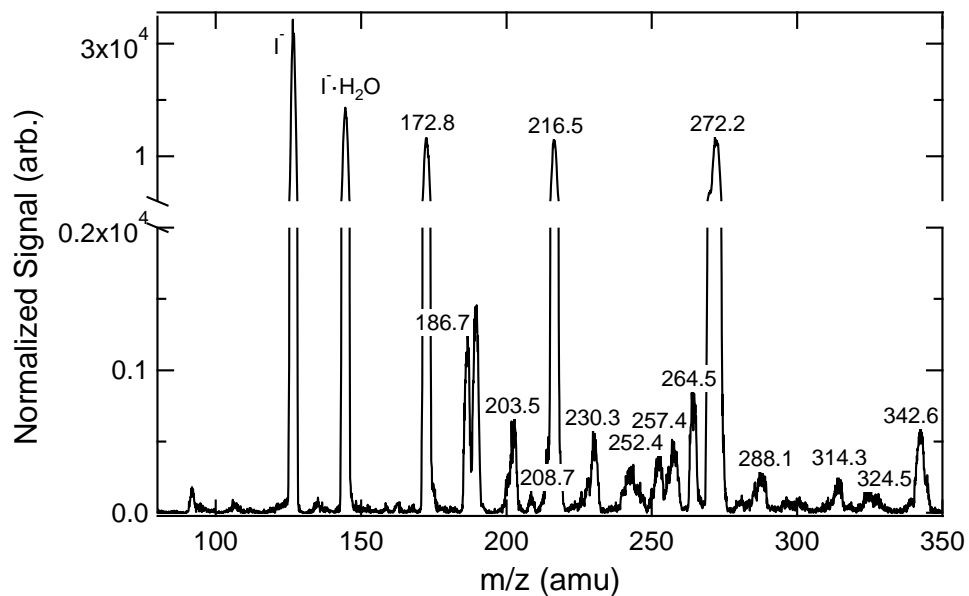
588

589

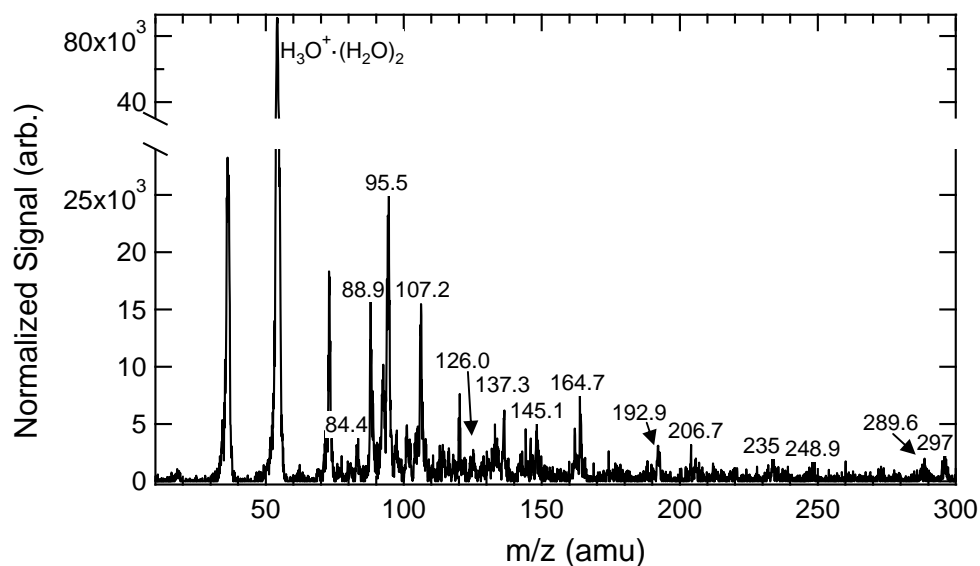
590



591
 592 **Figure 5.** Aerosol-CIMS spectra of atomized solutions of 0.2 M formaldehyde in 3.1
 593 M AS and H₂O. See the text for details of sample preparation and analysis. Negative-
 594 ion mass spectrum obtained using I⁻ as the reagent ion.
 595



596
 597 **Figure 6.** Aerosol-CIMS spectra of atomized solutions of 2 M formaldehyde/MG
 598 (1:1) in 3.1 M AS. See the text for details of sample preparation and analysis. Nega-
 599 tive-ion mass spectrum obtained using I⁻ as the reagent ion.
 600



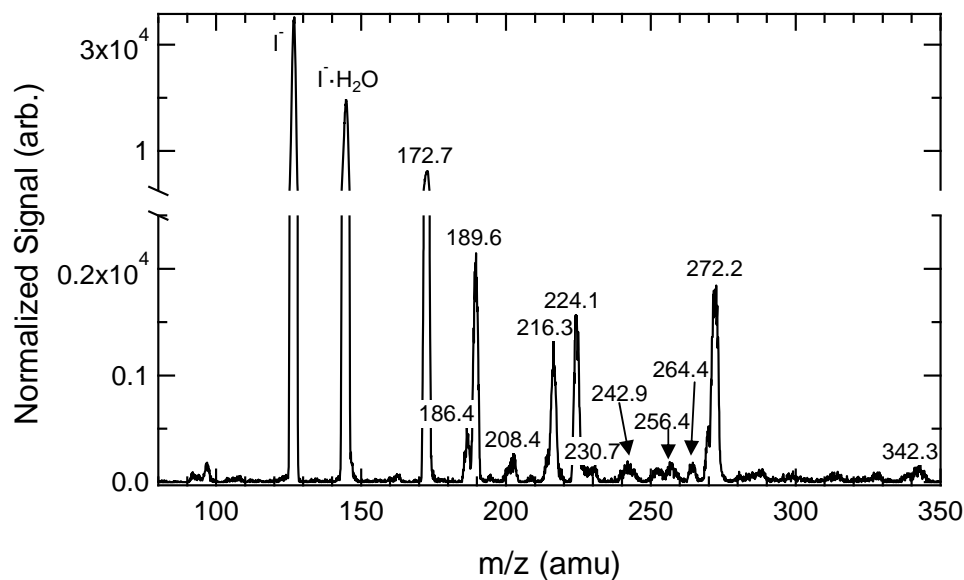
601

602 **Figure 7.** Aerosol-CIMS spectra of atomized solutions of 0.5 M acetaldehyde/MG

603 (1:1) in 3.1 M AS. See the text for details of sample preparation and analysis. Posi-

604 tive-ion mass spectrum using $\text{H}_3\text{O}^+(\text{H}_2\text{O})_n$ as the reagent ion.

605



606

607 **Figure 8.** Aerosol-CIMS spectra of atomized solutions of 2 M acetaldehyde/MG (1:1)

608 in 3.1 M AS. See the text for details of sample preparation and analysis. Negative-ion

609 mass spectrum obtained using I^- as the reagent ion.

610